# Appendix Data for

# The IFT81-IFT74 complex enhances GTP hydrolysis to inactivate RabL2 during intraflagellar transport

Niels Boegholm[1&], Narcis A. Petriman[1&], Marta Loureiro-López[2], Jiaolong Wang[1], Miren Itxaso Santiago Vela[1], Beibei Liu[3], Tomoharu Kanie[3,4], Roy Ng[4], Peter K. Jackson[4,5], Jens S. Andersen[2] and Esben Lorentzen[1,*]

[1] Department of Molecular Biology and Genetics, Aarhus University, Universitetsbyen 81, 8000 Aarhus C, Denmark

[2] Department for Biochemistry and Molecular Biology, University of Southern Denmark, Campusvej 55, 5230 Odense M, Denmark

[3] Department of Cell Biology, University of Oklahoma Health Science Center, OK, 73104, USA

[4] Baxter Laboratory, Department of Microbiology & Immunology, Stanford University School of Medicine, Stanford, CA 94305, USA

[5] Department of Pathology, Stanford University School of Medicine, Stanford, CA, 94305, USA

* Corresponding author, E-mail: el@mbg.au.dk

[&] These authors have contributed equally

**Contents**

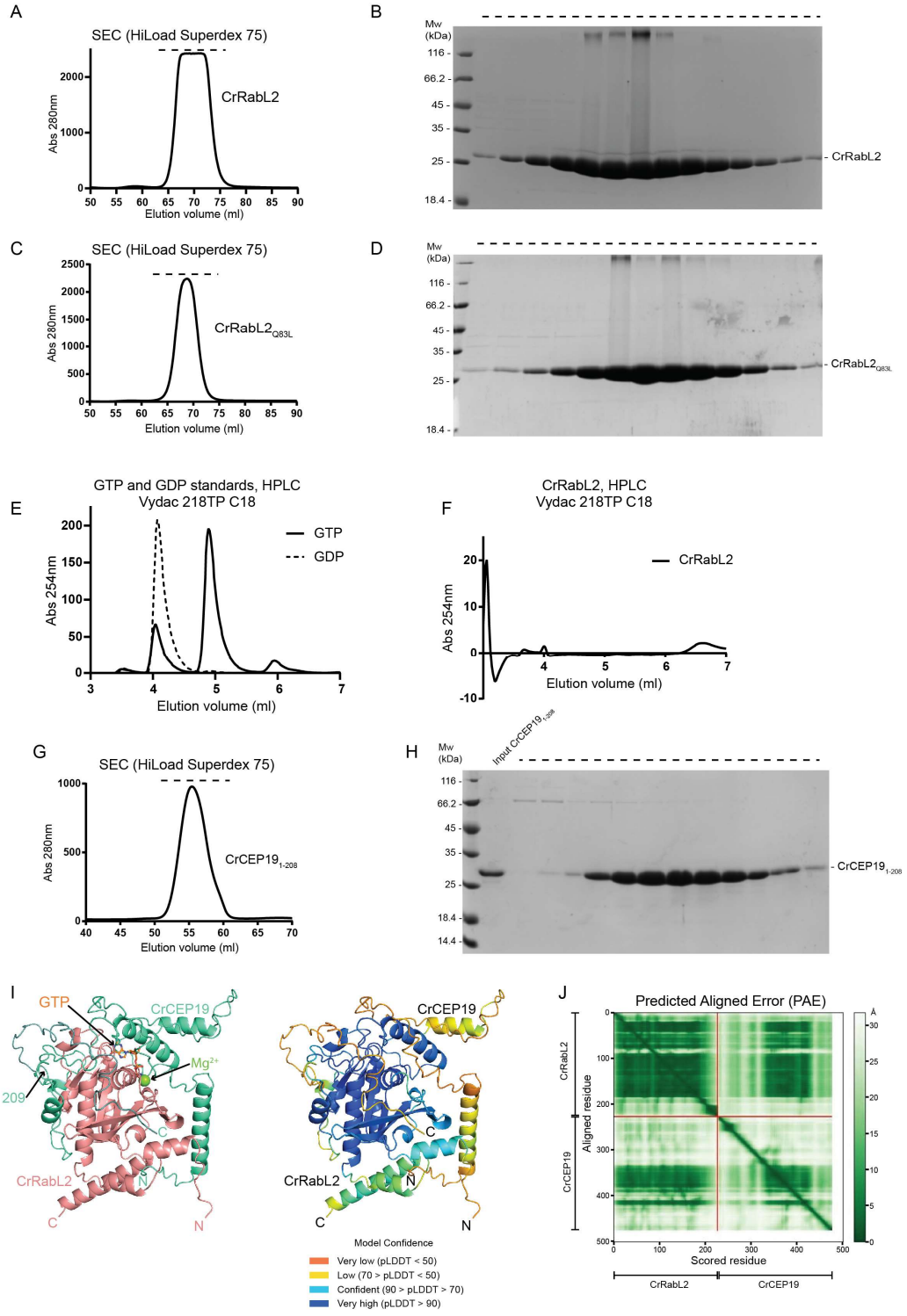


**Appendix Figure S1: CrRabL2 and CEP19 protein purification and their interaction as predicted by AlphaFold**

**(A)** SEC profile of purified CrRabL2. **(B)** The peak fraction highlighted with a top dashed line are verified for purity on SDS PAGE and stained with Coomassie. **(C)** SEC profile of $CrRabL2_{Q83L}$ mutant displaying a similar elution pattern to WT CrRabL2. **(D)** The SEC fractions highlighted with a top dashed line are verified for purity on SDS PAGE and stained with Coomassie. **(E)** High-performance liquid chromatography (HPLC) analysis showing the elution of GTP (solid line) and GDP (dashed line) standards on a Vydac 218TP C18 column. **(F)** HPLC run of purified CrRabL2 demonstrating that the protein does not co-purify with GDP or GTP nucleotides. **(G)** SEC profile of purified $CrCEP19_{1-208}$. **(H)** The SEC $CEP19_{1-208}$ fractions marked by a top dashed line in (G) are migrated on SDS PAGE and stained with Coomassie. **(I)** AlphaFold predicted structural model of CrRabL2 (colored salmon) in complex with CEP19 (green) is shown as cartoon representation on the left. The GTP as well as the position of $Mg^{2+}$ is modelled in the structure after superimposition with the Rab8-GppNHp (PDB code 4LHW). The right panel shows the CrRabL2-CEP19 complex colored according to the pLDDT score. **(J)** The plot displays the predicted alignment errors (PAE) on a residue basis for the AlphaFold model shown in panels (I) demonstrating confidence in the relative position of subunits within the complex. The Y-axis show aligned residues and the X-axis show the scored residues. The aligned error is color coded according to the bar to the right of the plots.

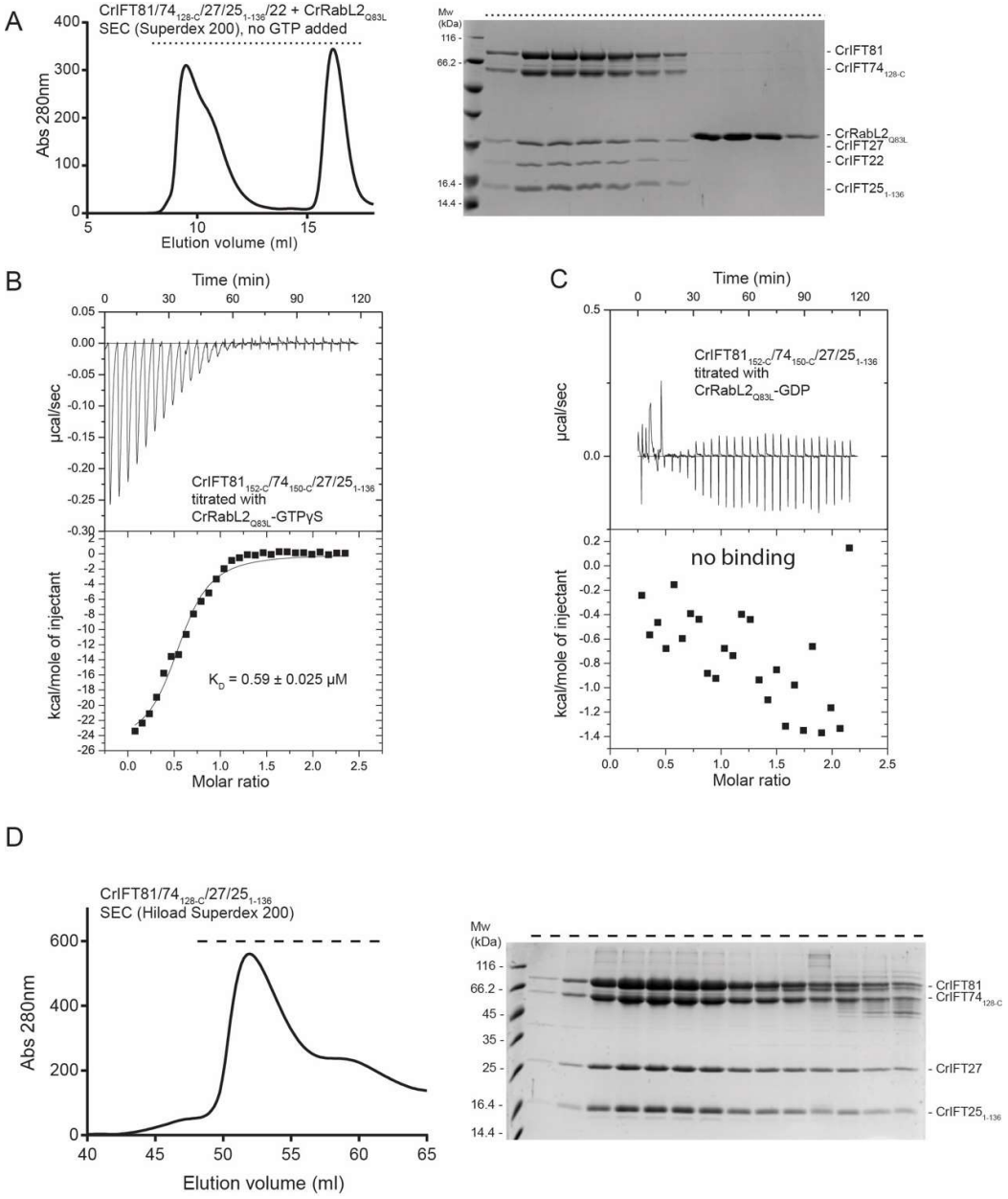


**Appendix Figure S2: RabL2 binds the IFT-B1 tetramer or pentamer only in the presence of GTP**

**(A)** Size exclusion chromatogram (left panel) and the corresponding SDS-PAGE gel (right panel) showing that CrRabL2$_{Q83L}$ cannot form a complex with CrIFT81/74$_{128\text{-}C}$/27/25$_{1\text{-}136}$/22 in the absence of GTPγS. The dashed lines above chromatograms indicate the SEC fractions migrated on SDS-PAGE and stained with Coomassie Brilliant blue. **(B)** ITC measures micromolar affinities of RabL2$_{Q83L}$ for the IFT81$_{152\text{-}C}$/74$_{150\text{-}C}$/27/25$_{1\text{-}136}$ complex in the presence of GTPγS. $K_D$ represents the average dissociation constant in µM calculated from three technical replicates. **(C)** No binding is observed for

RabL2$_{Q83L}$ to the IFT81$_{152\text{-}C}$/74$_{150\text{-}C}$/27/25$_{1\text{-}136}$ complex in the presence of GDP using ITC. **(D)** SEC profile of IFT-B1 tetramer purification (left) with the corresponding Coomassie stained SDS-PAGE gel (right). This sample is used for the GTPase assay shown in Fig. 2E-H.

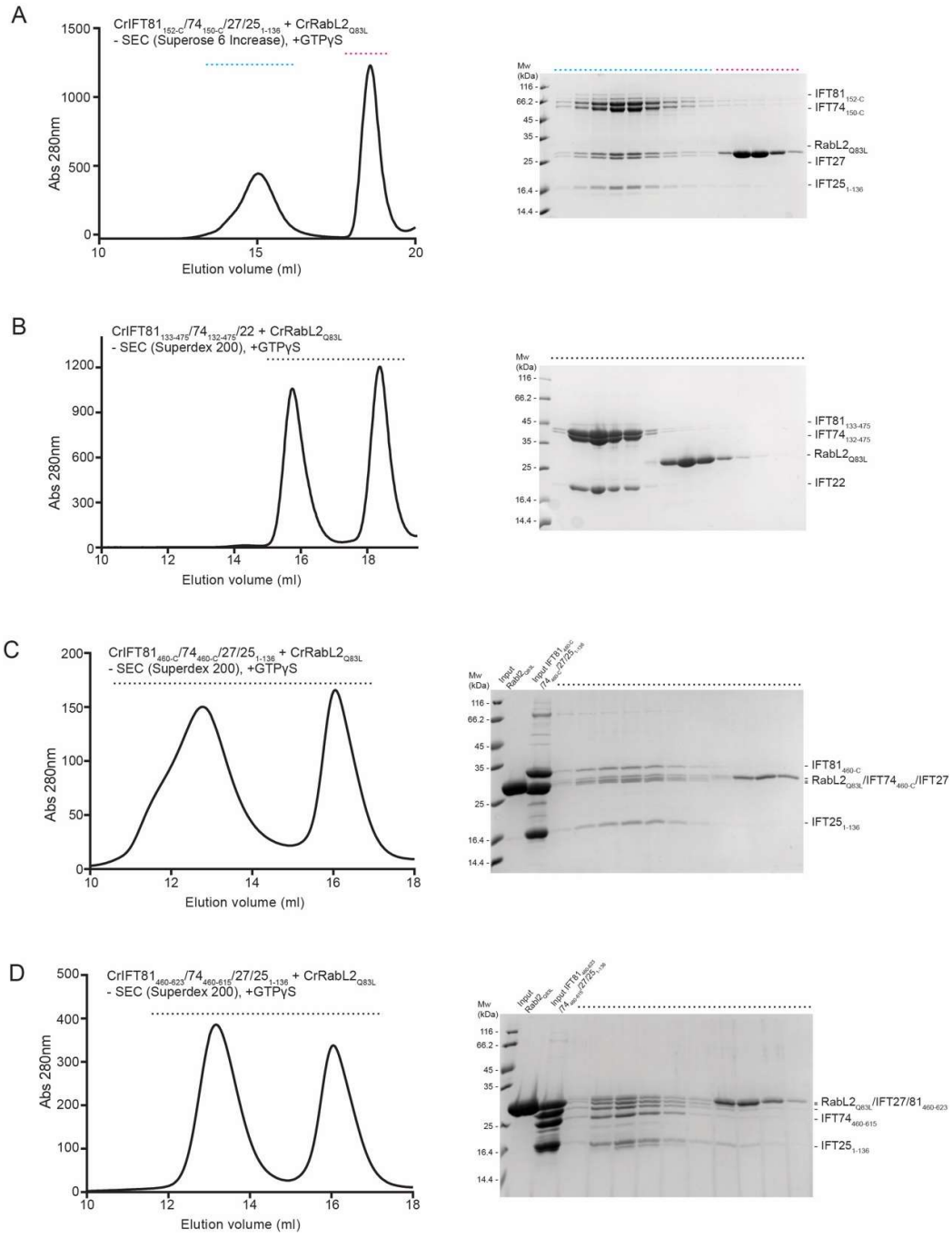


**Appendix Figure S3: CrRabL2 associates with the C-termini of the CrIFT81/74 complex**

**(A)** A size exclusion chromatogram (left) and the corresponding SDS-PAGE gel (right) that depicts complex formation between $CrRabL2_{Q83L}$ and a tetrameric $CrIFT81_{152\text{-}C}/74_{150\text{-}C}/27/25_{1\text{-}136}$ complex. The dashed lines indicate the SEC exclusion fractions investigated on SDS-PAGE (right) and stained with Coomassie. **(B)** Size exclusion chromatogram (left panel) and the corresponding SDS-PAGE gel (right panel) showing that $CrRabL2_{Q83L}$ cannot form a complex with $CrIFT81_{133\text{-}475}/74_{132\text{-}475}/22$. The

Coomassie staining on the right shows the composition of the highlighted SEC fractions (horizontal top dashed line on the left). **(C)** SEC profile indicating binding of $CrRabL2_{Q83L}$ to a $CrIFT81_{460\text{-}C}/74_{460\text{-}C}/27/25_{1\text{-}136}$ complex. Samples collected from the highlighted SEC fractions (dashed line) are migrated on SDS PAGE and stained with Coomassie (right panel). **(D)** Binding between $CrRabL2_{Q83L}$ and a $CrIFT81_{460\text{-}623}/74_{460\text{-}615}/27/25_{1\text{-}136}$ in the presence of GTPγS observed on SEC. The SEC fractions marked with a dashed line are monitored on SDS PAGE and stained with Coomassie on the right panel. All SEC runs shown in this figure were in the presence of 1mM of the non-hydrolysable GTP analogue GTPγS.

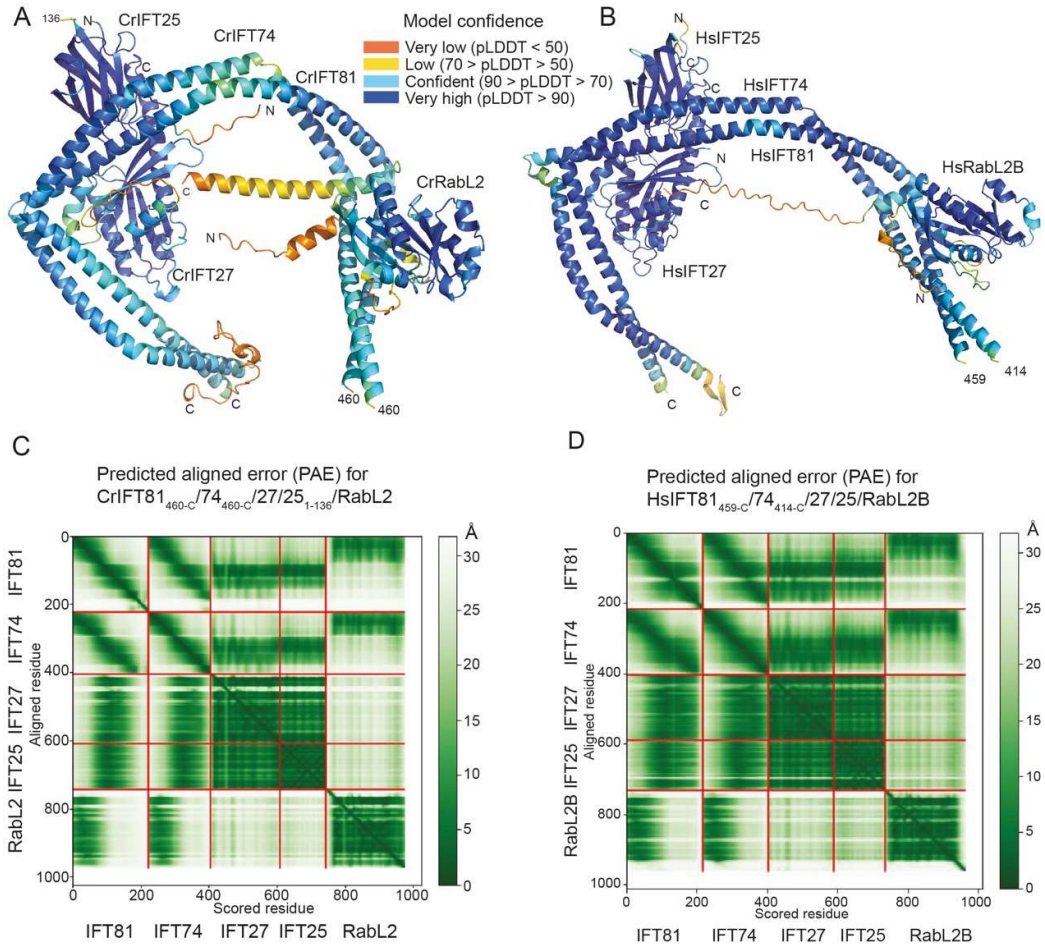


**Appendix Figure S4: (A, B) The AlphaFold models of Cr (A) and Hs (B) minimal IFT81/74/27/25/RabL2 complexes in the same orientation as shown in Fig. 4A-B.**

The structural models are colored by the per-residue estimate pLDDT confidence score. **(C, D)** The plots display the PAE for the AlphaFold models shown in panels (A) and (B) demonstrating confidence in the relative position of subunits within the complex. The Y-axis show aligned residues and the X-axis show the scored residues. The aligned error is color coded according to the bar to the right of the plots.

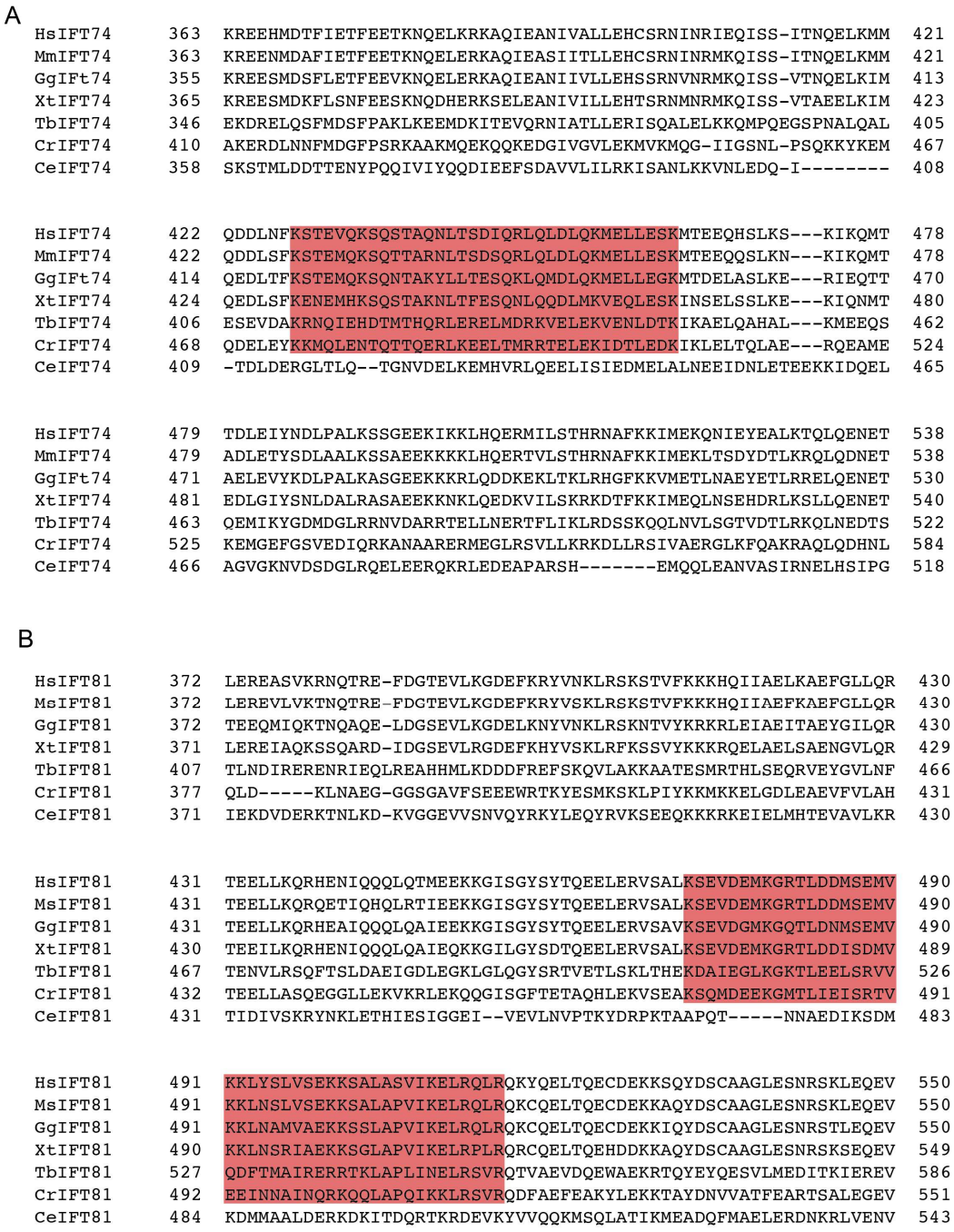


**Appendix Figure S5: Multiple sequence alignments of IFT74 and IFT81 homologues**

Sequence alignment of the C-terminal parts of IFT74 **(A)** and IFT81 **(B)** homologues from Hs (*Homo sapiens*), Mm (*Mus musculus*), Gg (*Gallus gallus*), Xt (*Xenopus tropicalis*), Tb (*Trypanosoma brucei*), Cr (*Chlamydomonas reinhardtii*) and Ce (*Caenorabditis elegans*). RabL2 interacting regions are marked in red.

A Inference of CRISPR Edits (ICE) Analysis of IFT74 KO clone 1

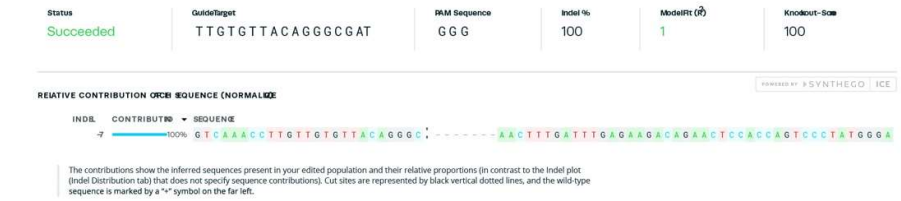


B

| Ciliation Assay<br>Two way ANOVA with Tukey's test | P value<br>24 hr s.s. | 48 hr s.s. | 72 hr s.s. |
|---|---|---|---|
| sgSafe+empty v.s. IFT74 KO+empty | 0.0014 | <0.0001 | 0.0001 |
| sgSafe+empty v.s. IFT74 KO+FLAG-IFT74 WT | 0.9887 | 0.9779 | 0.8101 |
| sgSafe+empty v.s. IFT74 KO+FLAG-IFT74 T438R | 0.0002 | 0.0195 | 0.0269 |
| IFT74 KO+empty v.s. IFT74 KO+FLAG-IFT74 WT | 0.0167 | 0.0003 | <0.0001 |
| IFT74 KO+empty v.s. IFT74 KO+FLAG-IFT74 T438R | 0.1961 | 0.3252 | 0.1915 |
| IFT74 KO+FLAG-IFT74 WT v.s. IFT74 KO+FLAG-IFT74 T438R | 0.0136 | 0.0142 | 0.0279 |

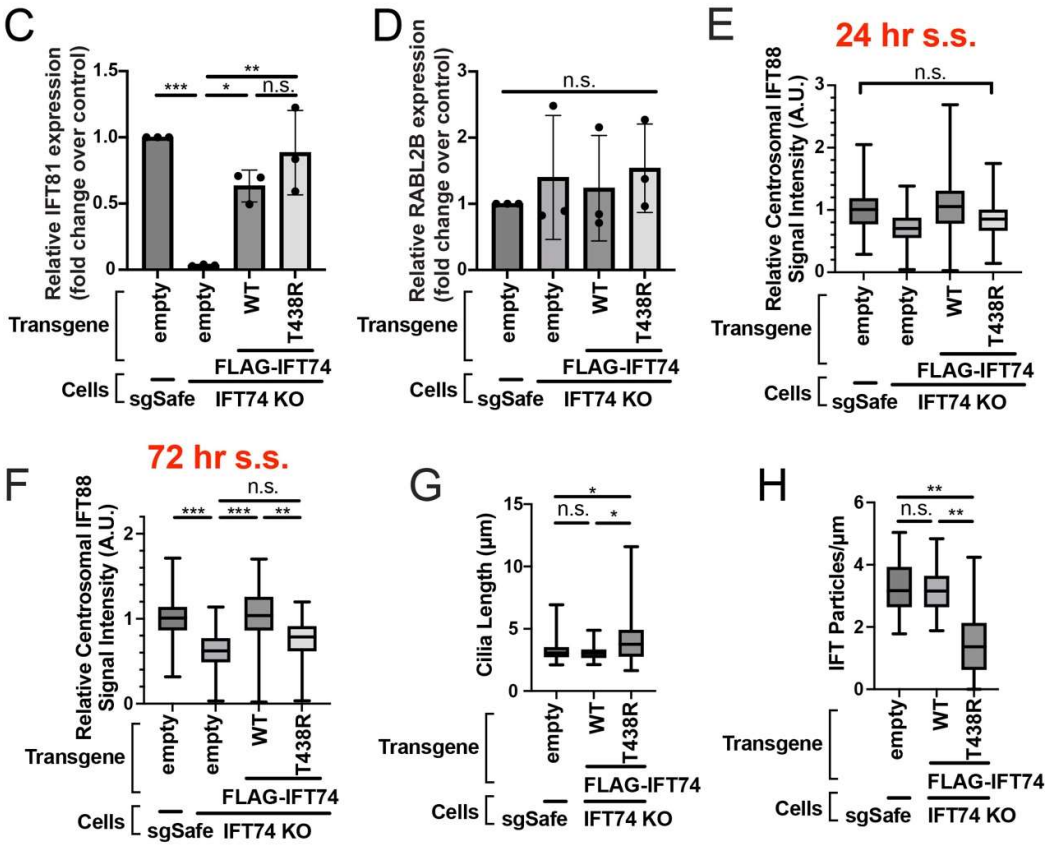


**Appendix Figure S6: CRISPR generated IFT74 KO cells**

**(A)** A summary of Inference of CRISPR Edits (ICE) Analysis of single cell clones of IFT74 KO cells.

**(B)** Statistical analysis of the time course of cilium formation assay shown in Fig. 6D. Data are averaged from three independent experiments. (**C-D**). Quantification of the immunoblots shown in Fig. 6E. Data

are combined from three independent experiments. Error bars represent ± SD. Statistics obtained through one-way analysis of variance (ANOVA) with Tukey's multiple comparison test. **(E-F)** Box plots showing centrosomal signal intensity of IFT88 in control (sgSafe) and IFT74 KO RPE cells with indicated transgenes serum starved (s.s.) for 24h (E) and 72h (F). The relative signal intensity compared with the average of the control (sgSafe + empty) are shown. Data are combined from three independent experiments: (E) n=129, 136, 81, (sgSafe + empty); 94, 166, 187 (IFT74 KO + empty); 81, 139, 183 (IFT74 KO + FLAG-IFT74 WT); 84, 136, 129 (IFT74 KO + FLAG-IFT74 T438R), (F) n=145, 142, 144 (sgSafe + empty); 141, 208, 144 (IFT74 KO + empty); 142, 135, 162 (IFT74 KO + FLAG-IFT74 WT); 108, 158, 167 (IFT74 KO + FLAG-IFT74 T438R). **(G)** Box plots showing cilia length from the immunofluorescence experiments shown in Figs. 6J-K. The data combined from three independent experiments. Cilia length of individual cells in each experiment are available from Figs. S7B, E, and H. **(H)** Box plots showing the number of IFT88 particles per μm of cilium from the immunofluorescence experiments shown in Figs 6J and K. Data are combined from three independent experiments. IFT particles per μm in individual cells in each experiment are available from Figs. S7C, F, and I.

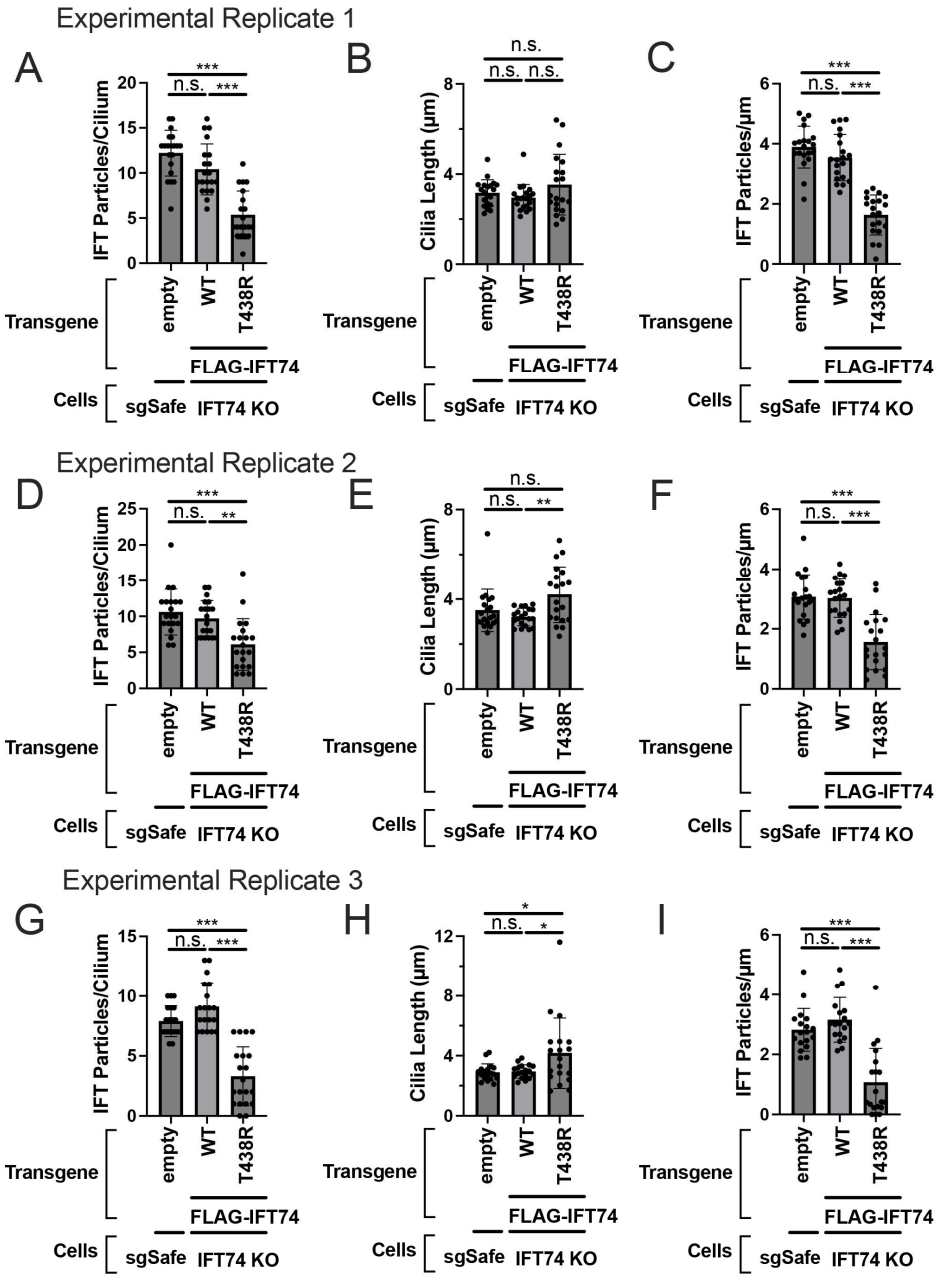


**Appendix Figure S7: Experimental replicates for data shown in Figure 6 and Appendix Figure S6**

**(A-I)** The number of IFT particles per cilium (A, D, and G), cilia length (B, E, and H), and IFT particles per µm of cilium (C, F, and I) in individual cells in each of the three experimental replicates. Each black dot indicates the value from each individual cell.